Evaluation of Workspace for Parallel Manipulators

Yoshito TANAKA, Isao YOKOMICHI and Junko ISHII

Abstract

Currently, there has been an increasing interest in the design of parallel machines. For construction machines, parallel chains are useful for the end effecter when combined with serial chains of construction machines as hybrid serial-and-parallel manipulators. They consist of a fixed base, a platform, and actuators, i.e., hydraulic power cylinders especially for harsh payload. The platform makes a 6DOF movement by controlling the length of the cylinders, while the workspace changes variously with orientation of a platform. This paper presents a method to search workspace of the manipulator for the efficient design and working capability using the 3D visualization technique. The device is expected to have as much as large workspace by reducing interference between links by constraining its motion. In order to search the workspace, geometric approach based on the inverse kinematics is employed. The solution of the inverse kinematics problem developed can be applied to describe the workspace. The boundary of the workspace is attained whenever at least one of the actuators reaches one of its limits. These limits for the six cylinders circumscribe the whole portion of the 3D Cartesian space for a specified orientation of the platform. Geometrical results are shown to be coincident to the experiments. The workspace plots are created with OpenGL and Visual C++ by implementation of the search algorithm. The real-time coordination of the workspace and the spatial movement of the manipulator will be demonstrated.

Keywords: Parallel-manipulator, Workspace, Serial-parallel, Inverse kinematics, Application module, Construction

1. Introduction

Parallel kinematic manipulators offer several advantages over their counterparts for certain applications. Among the advantages are greater load carrying capacities, higher stiffness, and reduced sensitivity to certain errors. Stewart type of parallel mechanisms is one of parallel manipulators that are used increasingly in manufacturing, inspection and research [1], [2]. However, these machine's non-intuitive kinematics, workspace, and error characteristics create obstacles to industry's acceptance [3]. As to the workspace restrictions due to limited strut lengths have been considered based on geometrical properties of the workspace [4], [5]. Other important constraints, such as joint angles and avoiding strut collisions were integrated into workspace modelling to verify the trajectory within the workspace [6].

In this paper, with intension of construction machine design, geometrical analysis for computing the workspace of 6DOF Stewart manipulators is presented using inverse kinematics when only the constraints on the strut limits are considered. In practice, the workspace producing large range of orientation can be regarded as being useful; hence the workspace has been examined for desired orientations with large rotation angles of the platform. In the workspace analysis 2D plots of boundary curves in XY plane are used to construct the whole workspace. To confirm the real-time visualization of the workspace and to understand the motion capabilities of a prototype machine, an application module is developed which simultaneously displays motions and workspace of the manipulator in 3D images. Since the motion and the workspace are too complex to gain an immediate understanding of their correlation, the module may be useful to create the spatial motion of the virtual prototype machine and estimate a real-time workspace boundary.

2. Workspace Analysis

2.1 Kinematics of the Parallel Manipulator

The workspace of the parallel manipulator can be described as the set of all spatial coordinate points of the center of the platform with a given orientation of the platform. The workspace of parallel manipulators is limited owing to three types of constraints: 1) mechanical limit on the passive joints; 2) interference between links; and 3) limited range in the length of linear actuators (cylinders). The prototype (Fig.1) has no mechanical limits on joints and interference between links within the range in the length of cylinders. Hence, the geometrical analysis for computing the workspace will be described when only the length limits of cylinders are considered.

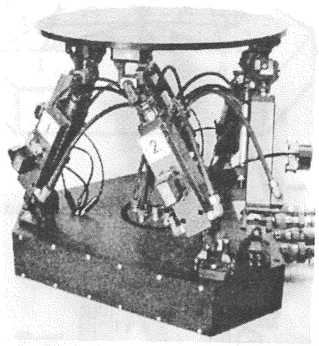

Fig.1 Stewart platform-based manipulator

The parallel manipulator, whose design is based on the Stewart Platform mechanisms, comprises a platform, six cylinders and a base. Six cylinders, each of which is composed of a hydraulic actuator (Fig.2), link the platform and base together. Driving the servo to shorten or extend cylinder lengths produces motion of the platform. Figure 3 illustrates the diagram of the link-space control scheme

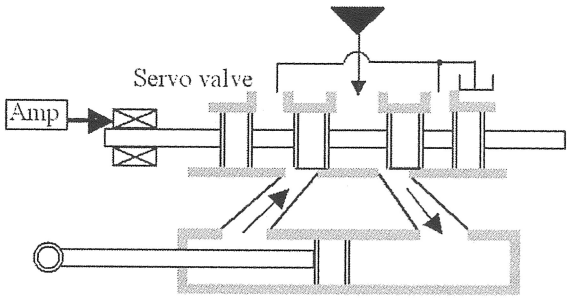

Fig.2 Hydraulic actuator

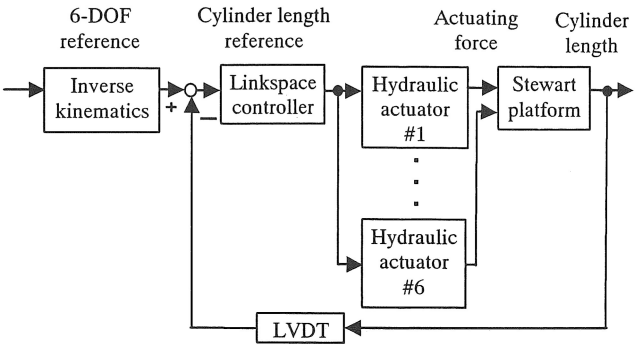

Fig.3 Control methods

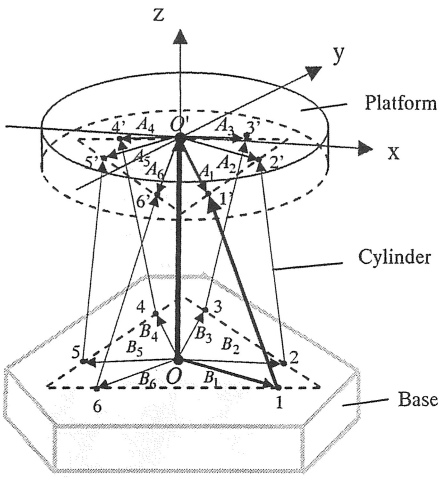

Fig.4 Platform frame assignment

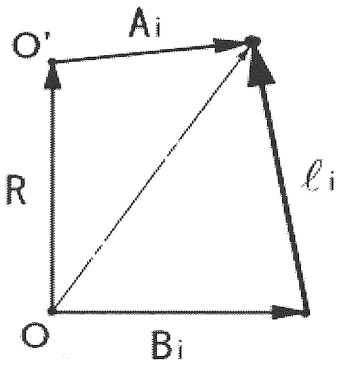

Fig.5 Vector diagram for the cylinder

(semi-closed) of the manipulator. The 6 DOF reference is transformed into desired cylinder lengths using inverse kinematics, which is compared with the cylinder lengths measured by LVDT sensors. The proportional scheme controls the servo valves (Fig.2).

This section will use vector algebra to attain a closed-form solution for the inverse kinematics.

The inverse kinematics of the parallel manipulator can be formulated so as to determine the required cylinder vector for a given orientation of the platform with respect to the base. Figure 4 shows that two coordinate frame {A} and {B} are assigned to the platform and the base of the manipulator, respectively. The origin of frame {A} is at the centroid O' of the platform, while the frame{B} has its origin at the centroid O of the base. The pose of the platform is specified by rotation of frame {A} and the position of the centroid O' with respect to the frame {B}. We proceed to consider the vector diagram for the i-th cylinder given in Fig.5. The position of the centroid O' is represented by vector $R=(x, y, z)^T$ with respect to frame {B}. Furthermore, if vector **Ai** describes the position of the attachment point of the cylinder on the platform with respect to frame {B}, and vector **Bi** the position of the attachment point on the base, then the cylinder vector and its Euclidean norm expressed with respect to frame {B} can be computed by

$$\ell_i = A_{im} T + R - B_i \tag{1a}$$

$$L_i = \|\ell_i\| = \|A_{im} T + R - B_i\| \tag{1b}$$

where **Aim** describes the attachment point of the cylinder on the platform relative to frame {A} and T represents the orientation matrix of the platform which can be expressed with roll-pitch-yaw angles as ϕ, θ, and φ by

$$T = \begin{pmatrix} 1 & 0 & 0 \\ 0 & \cos\phi & \sin\phi \\ 0 & -\sin\phi & \cos\phi \end{pmatrix} \begin{pmatrix} \cos\theta & 0 & -\sin\theta \\ 0 & 1 & 0 \\ \sin\theta & 0 & \cos\theta \end{pmatrix} \begin{pmatrix} \cos\varphi & \sin\varphi & 0 \\ -\sin\varphi & \cos\varphi & 0 \\ 0 & 0 & 1 \end{pmatrix} \tag{2}$$

Equations (1a) and (1b) represent the closed-form solution to the inverse kinematics problem in the sense that required cylinder length Li={L} (i=1,2...6) can be computed to yield a given pose of frame {A}.

2.2 Numerical Methods

The solution of the inverse kinematic problem developed above can be used to describe the workspace of the parallel manipulator. If the mechanical interference is neglected, the boundary of the workspace is attained whenever at least one of the cylinders reaches one of its limits. If the range of motion of the cylinders given by Eq. (1b) satisfies

$$Lmin < Li < Lmax,\ i=1, 2...6 \tag{3}$$

then vector **R** can describe the workspace for a specified platform orientation. A section of the workspace can be obtained on planes parallel to the xy plane as show in Fig. 6.

For a $x_j y_j$ plane with $z=z_j$, vector **R** (i, j) is defined in the form

$$R(i, j) = (r_i \cos\alpha_i, r_i \sin\alpha_i, z_j + R_0) \tag{4}$$

where r_i and α_i are treated as a polar coordinate, and R_0 is the distance between O-O' when the pose of the platform is neutral position. The process of searching the boundary of workspace on $x_j y_j$ plane is accomplished by rotating the radius r_i for every finite interval: $0 \le \alpha_i \le 2\pi$, and $z_{min} \le z_j \le z_{max}$ using relations (1b), (2), and (4). The algorithm is the following. Taking a polar angle α_i in the section and drawing a polar line r_i, the intersection point between

the line r_i and the boundary curve of the workspace in this section can be obtained.

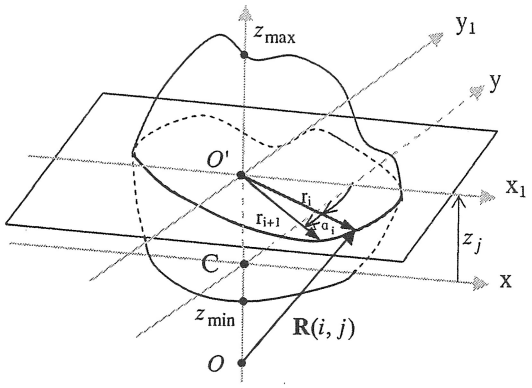

Fig.6 Determination of the boundary in xy plane

2.3 Geometric Description of the Workspace

The required cylinder lengths can be directly computed from Eq. (1b) for given values of the position of joints on the base and on the platform, and for prescribed values of a pose of the platform. If the range of motion of the cylinders is given by

$$L_{min} \le L_i \le L_{max} \qquad (5)$$

then the boundary of the workspace can be obtained geometrically as set of points with $L_i = L_{min}$ or $L_i = L_{max}$ which represent concentric spheres of radii L_{min} and L_{max} [7]. Hence, the workspace of the parallel manipulator can be described as the intersection of 6 regions, so each of these regions is the difference of two concentric spheres. If we desire to find the section of the workspace on a plane parallel to the xy plane defined as $z=z_j$ (z-level cutting plane), then the regions will be 6 pairs of concentric circles. The position of the centers of the circles will depend on the orientation specified for the platform and on the joint positions.

The workspace of the manipulator shown in Fig.1 will now be studied. Its geometric properties are summarized in Table1.

Table 1 Geometric properties of the prototype manipulator (all length are given in mm)

A_1	$(119.8127.5, -60.0)^T$	B_1	$(221.4, 40.0, 50.0)^T$
A_2	$(50.5, 167.5, -60.0)^T$	B_2	$(-76.0, 211.7, 50.0)^T$
A_3	$(-170.3, 40.0, -60.0)^T$	B_3	$(-145.3, 171.7, 50.0)^T$
A_4	$(-170., -40.0, -60.0)^T$	B_4	$(-145.3, -171.7, 50.0)^T$
A_5	$(50.5, -167.5, -60.0)^T$	B_5	$(-76.0, -211.7, 50.0)^T$
A_6	$(119.-127.5, -60.0)^T$	B_6	$(221.4, -40.0, 50.0)^T$
L_{max}	353.0	L_{min}	255.0

Figures 7, 8, 9 and 10 depict the trajectories of six cylinders in z-level cutting planes (z=0), (Fig. (a)) for reference orientations, as well as the corresponding workspace boundaries for various z-level cutting planes (Fig. (b)). Figures 7-10 (a) indicate how each of the lower and upper limits of the cylinder lengths contributes the workspace boundaries,

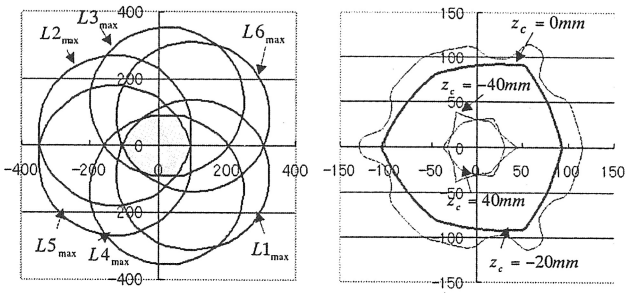

(a) Trajectory of 6 cylinders (b) Workspace boundary

Fig.7 2D Plots of workspace (Neutrality)

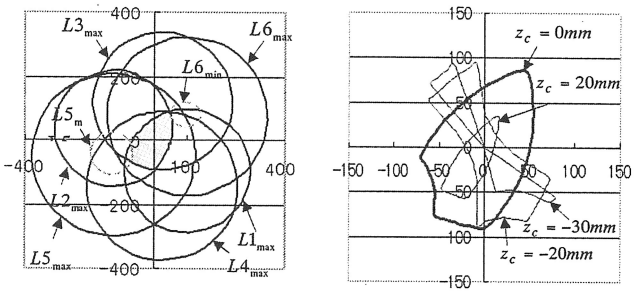

(a) Trajectory of 6 cylinders (b) Workspace boundary

Fig.8 2D Plots of workspace (roll: $\phi = 10°$)

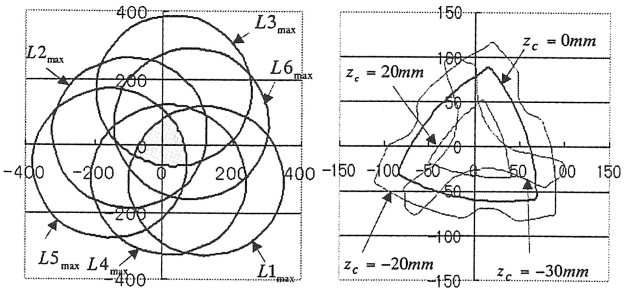

(a) Trajectory of 6 cylinders (b) Workspace boundary

Fig.9 2D Plots of workspace (pitch: $\theta = 10°$)

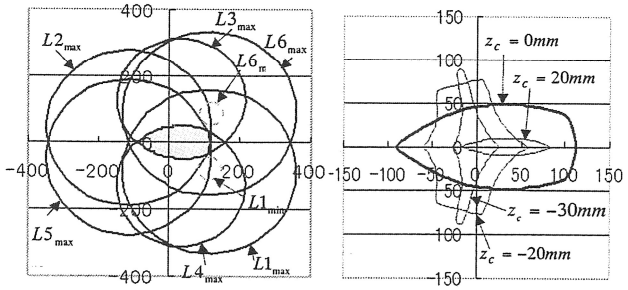

(a) Trajectory of 6 cylinders (b) Workspace boundary

Fig.10 2D Plots of workspace (yaw: $\varphi = 10°$)

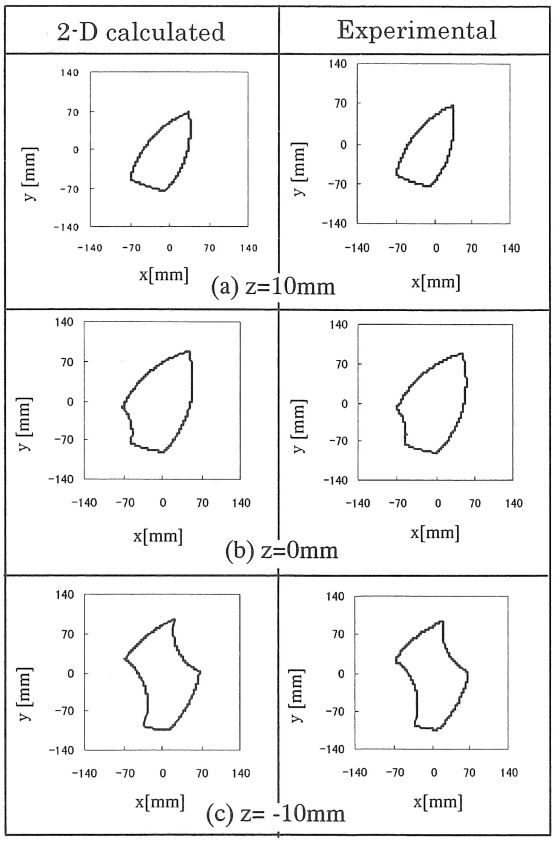

Fig.11 Comparison between calculation and measurements (roll: $\phi = 10°$)

depending on the orientations of the platform. Since all the inner and outer regions of the circular arcs defined, respectively by Li_{max} and Li_{min}, comprise the reachable space (the enclosed areas), the circular arcs located inside all the internal (Li_{max}) and external circles (L_{min}) constitute the boundary of the workspace.

It is noted that the boundaries of the workspace are depend only on circular arcs of six L_{max}'s for the three reference orientations, except one (Fig.8 (a)) where the outer circular arcs of $L5_{min}$ contributes the boundary of the workspace. On the other hand, the level curve of the workspace boundary away from neutrality level (z=0) varies in shape and area, due to the constraints of lower limits of cylinder lengths Li_{min} (Figs.7-10 (b)).

Figure 11 shows the workspace on z-cutting planes as platform rolls at $\varphi = 10°$ in comparison with the measurements. In experiments, the working points were measured by PSD camera that scans the displacement of z-level as the platform rolls, and the agreement between the calculation and measurement is good. In view of the preceding discussion this geometrical treatment has advantages, in terms of convergence and solution tolerance, over the conventional approach[8] that uses iteration technique to compute the workspace boundaries. Since the workspace and motion of the manipulator are too complex to gain an immediate understanding of their correlation, we develop an application module in Visual Basic environment, which simultaneously displays the motions and its workspace of the parallel manipulator in 3D images.

3. 3D display of workspace of manipulator

3.1 Construction of 3D display program system

The above presented algorithms for estimating the workspace of the parallel manipulator were first implemented in the C++ (VC++) programming language and tested to graphically display the motion and workspace using OpenGL.

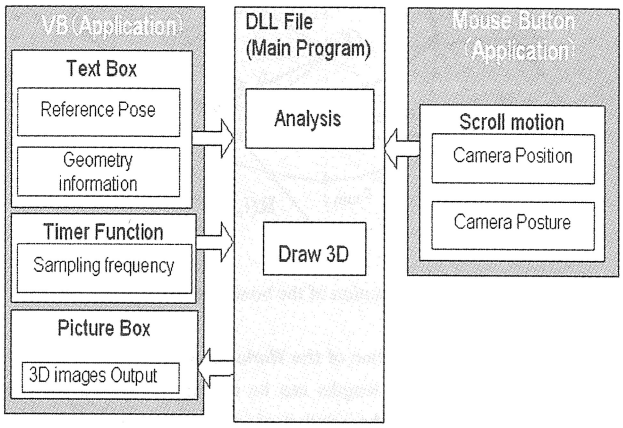

Fig.12 Main modules of Application

The program was then defined as DLL function that executes the operation shown in Fig.12. The DLL was incorporated and declared into the Visual Basic (VB) program as a visualization tool that simulates the motion of the mechanism and displays its workspace simultaneously. The procedure followed to obtain a real-time workspace and the spatial movement of the parallel manipulator is the following. For a set of pose of the 6 degree-of-freedom, i.e., $(x_r, y_r, z_r, \phi_r, \theta_r, \varphi_r)$, first the reference vector **R** (Eq. (4)) will generate the cylinder vector, the configurations of the platform and the cylinder.

Then the workspace vector **R** successively calculates the arbitrary point on z-level cutting plane that satisfies the constraint conditions under the same set pose. The new configuration of the mechanism corresponding to the point **R** will be created for the graphical presentation on the picture box of VB. This computation process has been ported to the VB environment for a real-time coordination of workspace and spatial movement of the mechanism.

3.2 Details of processing 3D-workspace display

It is obvious from experiments that the actual workspace of the manipulator constitutes smooth surfaces. In analysis, the workspace vector **R** is estimated for the discrete values of rotation angle α and z level, i.e., $\Delta\alpha$ and Δz, which results in discrete vector **R** (i, j). To construct the smooth surface of vector **R** whose coordinate is given by x_{ij}, y_{ij}, z_{ij}, two triangle planes and are generated for the vectors **R** (i, j), **R** (i, j+1), **R** (i+1, j+1), and **R** (i+1, j), as shown in Fig.13. The corresponding OpenGL commands are given in the following listing code.

PROGRAM LISTING

```
// drawing of triangle
glBegin (GL_POLYGON);
```

glVertex3d (x_{ij}, y_{ij}, z_{ij});
glVertex3d ($x_{i+1,j+1}$,$y_{i+1,j+1}$,$z_{i+1,j+1}$);
glVertex3d ($x_{i+1,j}$, $yi_{+1,j}$,$z_{i+1,j}$);
glEnd ();
// drawing of triangle
glBegin (GL_POLYGON);
glVertex3d (x_{ij}, y_{ij}, z_{ij});
glVertex3d ($x_{i,j+1}$,$y_{i,j+1}$,$z_{i,j+1}$);
glVertex3d ($x_{i+1,j+1}$,$y_{i+1,j+1}$,$z_{i+1,j+1}$);
glEnd ();

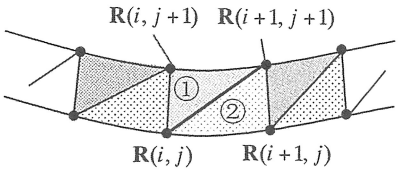

Fig.13 Surface triangular planes

Figure 14 shows the main screen developed with OpenGL technology for the 3D visualization of the workspace. The main function of this system is summarized as follows:

1) The main screen for 3D display was designed with VB that facilitates inclusion of controls. The screen displays the 3D workspace and includes the control for data settings, where design parameters such as platform geometry and cylinder location as well as the 6DOF poses of the manipulator can be easily set.

2) The display screen can be turned on and off at every 0.01s using PC with clock 2.8GHz, which provides enough speed to view the variation of workspace and continuous motion of the platform in a lifelike virtual reality environment. At the same time, 6DOF poses can be read in screen when the workspace is displayed in real time.

3) The generated 3D workspace can be rotated around the 3 axes, and translated in perspective for better visualization of the details by scrolling mouse (Mouse Button Application).

Figure 15 shows an example view of workspace in 3-view mode when the platform is set at the neutral position.

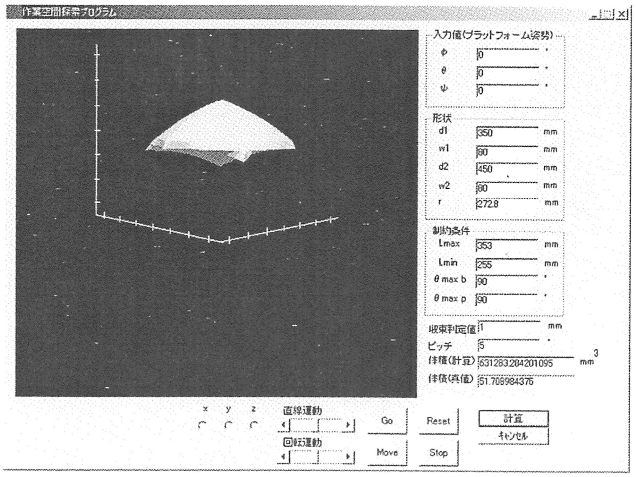

Fig.14 Main screen

Figure 16 shows the effect of the platform pose on the workspace of the parallel manipulator under study. For a neutral position, the maximum cylinder lengths mainly define the upper half of the workspace, while the middle section of the workspace is free from the joint angle limits, and the bottom of the workspace is defined by minimum cylinder length. Figures 16 (a-1)-(a-2), (b-1)-(b-2), and (c-1)-(c-2) show the reduction of the workspace as the platform rolls, pitches, and yaws from 5 to 10 degrees, respectively.

The general shape is similar to the neutral pose, but the bottom section of the workspace is reduced considerably and the vertices disappear at bottom with increase in platform posses. Since the movement of the working point of the manipulator occurs in 3D space, the boundary of the accessible workspace is a 2D surface.

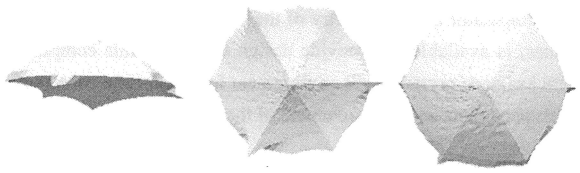

(a)View of side (b) View of bottom (c) View of top

Fig. 15 View of workspace

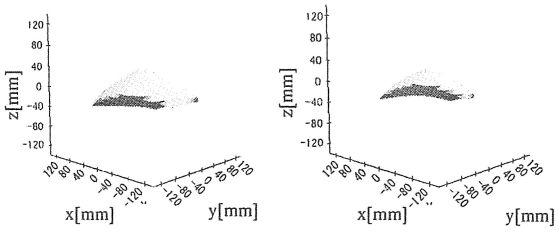

(a-1) f =5° (a-2) f =10°

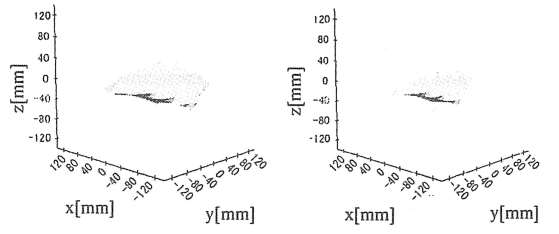

(b-1) θ=5° (b-2) θ=10°

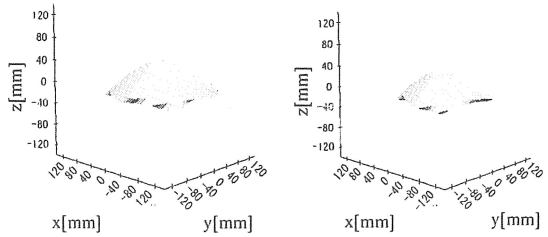

(c-1) ψ=5° (c-2) ψ=10°

Fig. 16 Effect of platform pose on the workspace configurations

4. Conclusions

The inverse kinematics for the workspace analysis of parallel manipulator has been formulated, and a geometrical algorithm to evaluate the workspace has been developed using search vector and trajectories of cylinders on the z-level cutting plane that precisely define the workspace boundaries. The workspace constraint is formulated in terms of the cylinder length, with the mechanical interference, such as angular limits and collision between links, neglected. Workspace plots show that as the platform orientation increases, the overall workspace decreases. And comparison of the numerical search with the measurements showed good agreement. Also, this numerical search method to generate workspace, together with mechanism motion developed, is generic to be applied to other parallel-serial manipulator if the geometry of the machine, such as construction machines, is available. To provide design efficiency this computation process has been ported to VB environment for a real-time coordination of workspace plots and the movement of the mechanism.

Acknowledgement

The research work reported in this paper is sponsored in part by the Japan Society for the Promotion of Science (JSPS) under Grant-in-Aid for Scientific Research (C), No.20500500.

References

[1] C. Nguyen, S. Antrazi, L. ZhouK, and E. Campbell, J. Robotic Systems, 10, No.5 (1993) 657.
[2] D. Liu, R. Che, and X. Luo, IEEE Transactions on Instrumentation and Measurement, 52, No.1 (2003) 119.
[3] T. Oiwa, Proc. 6th Int. Conference on Mechatronics Technology, (2002) 433.
[4] C. Gosselin, Transaction of the ASME, J. of Mechanical Design, 112 (1990) 331.
[5] C.M.Luh, F.A. Haug, and C.C.Qui, Transaction of the ASME, J. of Mechanical Design, 118 (1996) 220.
[6] M.k.Lee and K.W.Park, IEEE/ASME Transaction on Mechatronics 5, No.4 (2000) 367.
[7] D.F. Qiu, in: X.W. Yang, Y.Y. Chu, K.W. Sun (ed.), Proc. 4th Int. Symp. on East Asian Resources Recycling Technologies, Beijing, International Academic Publishers (1997) 93.
[8] J.P.Conti, C.M.Clinton, G.Zhang, and A.J.Waver-ing National Institute of Standards and Technology (NIST) 6135 (1998).

(2008年10月7日 受理)